THE JOURNAL OF PHYSICAL CHEMISTRY B

Article

pubs.acs.org/JPCB

# Salting-Out of Methane in the Aqueous Solutions of Urea and Glycine–Betaine

Mayank Kumar Dixit, Asrar A. Siddique, and B. L. Tembe*

Department of Chemistry, Indian Institute of Technology Bombay, Powai, Mumbai 400076, India

Supporting Information

**ABSTRACT:** We have studied the hydrophobic association and solvation of methane molecules in aqueous solutions of urea and glycine betaine (GB). We have calculated the potentials of mean force (PMFs) between methane molecules in water, aqueous GB, aqueous urea and aqueous urea–GB mixtures. The PMFs and equilibrium constants indicate that both urea and GB increase the hydrophobic association of methane. Calculation of thermodynamic parameters shows that the association of methane is stabilized by entropy whereas solvation is favored by enthalpy. In the case of the water–urea–GB mixture, both hydrophobic association and solvation are stabilized by entropy. From the investigation of radial distribution functions, running coordination numbers and excess coordination numbers, we infer that both urea and GB are preferentially excluded from methane surface in the mixtures of osmolytes and methane is preferentially solvated by water molecules in all the mixtures. The favorable exclusion of both urea and GB from the methane surface suggests that both urea and GB increase the interaction between methane molecules, i.e., salting-out of methane. We observe that addition of both urea and GB to water enhances local water structure. The calculated values of diffusion constants of water also suggest enhanced water–water interactions in the presence of urea and GB. The calculated free energies of methane in these mixtures show that methane is less soluble in the mixtures of urea and GB than in water. The data on solvation free energies support the observations obtained from the PMFs of methane molecules.

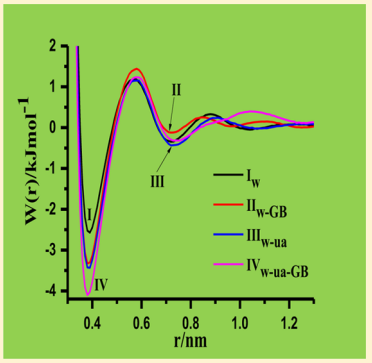


## 1. INTRODUCTION

Hydrophobic interactions among nonpolar groups play a significant role in the stabilization of folded states of biomolecules.[1−9] Osmolytes are small naturally occurring organic molecules having an ability to protect the living species against harsh environmental conditions.[10,11] Osmolytes are of two types: (a) protecting and (b) denaturing. Urea is a denaturing osmolyte whereas trimethylamine *N*-oxide (TMAO), glycine betaine (GB), sarcosine, and taurine are protecting osmolytes. The cellular proteins of marine fishes such as shark, skates, and rays contain high concentrations of these osmolytes to maintain suitable osmotic pressures. The high urea concentration drives the denaturation of proteins. There are two types of mechanisms to explain how urea denatures proteins: indirect mechanism and direct mechanism. In the indirect mechanism, it is proposed that urea molecules diminish the hydrophobic effect by altering water structure and thereby enhancing the solvation of hydrophobic groups.[12−18] The direct mechanism assumes that preferential interaction of urea with hydrophilic backbone as well as hydrophobic side chains of proteins is responsible for unfolding of proteins in aqueous urea solutions.[19−30]

Protecting osmolytes such as TMAO, glycine betaine, sarcosine, etc. provide stability to folded structures of proteins and cancel the denaturing effect of urea. It has been proposed that TMAO counteracts the denaturing effect of urea because of favorable exclusion of TMAO from protein backbone and strong interaction of TMAO with urea and water.[31−43] Recently, it has been reported that there is exclusion of urea and TMAO from an amino acid surface.[44] Because of preferential interaction of TMAO with water, urea molecules self-aggregate and are not available to solvate the amino acids.[44]

Bolen et al.[31−34] have analyzed the transfer free energies data and infer that in urea–TMAO mixtures, stabilization of a protein is because of the exclusion of osmolytes from its backbone and there is a negligible role of hydrophobic side chains in the stabilization of proteins. Horinek et al.[45] reported that transfer free energies of solutes from one solution to another are concentration scale dependent and have brought out the role of hydrophobic side chains, thereby, altering the interpretation of Bolen et al.

Like TMAO, glycine betaine is an important protecting osmolyte that cancels the denaturing effect of urea.[46] Narendra et al. have proposed that there are strong binding interactions between urea–GB, urea–urea, urea–water, and GB–water.[47] Therefore, urea molecules are not available to solvate the protein. In another paper, Kumar et al.[48] have shown that there are exclusions of GB from peptide surface due to enhanced interactions between urea–GB and water–water. These

**Special Issue:** Biman Bagchi Festschrift

**Received:** January 19, 2015
**Revised:** May 11, 2015





DOI: 10.1021/acs.jpcb.5b00556
J. Phys. Chem. B XXXX, XXX, XXX–XXX

enhanced interactions render urea unavailable for solvation of peptide.[48]

The structural studies and thermodynamic properties of hydrophobic surfaces for nonpolar molecules like methane in water and mixtures of osmolytes have been explored previously.[49−57]

It has been shown that the association of hydrophobic methane molecules is stabilized whereas the association of large nonpolar solutes is destabilized by urea.[49−51] Also, the clustering of methane is enhanced on the addition of urea into water because of preferential binding of methane with water.[52−54]

Garde et al.[55] have used the technique of MD simulations to show that there is no effect of TMAO on the hydrophobic phenomenon of methane molecules because enthalpy and entropy terms compensate each other. They have shown that contact minima between methane molecules are stabilized by entropy whereas solvent-separated minima are stabilized by enthalpy.[56] Paul et al.[57] have reported the salting-out (association) of methane in aqueous urea and that in aqueous TMAO solutions, TMAO has negligible effect on the hydrophobic association of methane. Therefore, it is of interest to study the effect of other mixed osmolytes on hydrophobic surfaces.

Because different combinations of osmolytes are present in the biological systems, the behavior of systems in the presence of mixed osmolytes needs to be understood in detail. In the present work, we have studied the effect of glycine betaine (GB) on the hydrophobic association and solvation of methane molecules in the aqueous solutions in the presence of urea molecules. We have computed the thermodynamic quantities ($\Delta G$, $-T\Delta S$, and $\Delta H$) at each methane−methane separation. We have also investigated the preferential solvation of methane molecules by water, GB, and urea in aqueous solutions of these osmolytes. We have calculated the solvation free energies and preferential binding constants of methane in water, aqueous GB, aqueous urea and aqueous urea−GB solutions and investigated the solubility and preferential binding of methane in these mixtures. We discuss the methodology and computational details in section 2. Our results are given in section 3, discussions are in section 4, and conclusions are given in section 5.

## 2. METHODOLOGY AND COMPUTATIONAL DETAILS

We have carried out classical MD simulations using the GROMACS package (version 4.6.4)[58] in four different solvent systems: water, aqueous urea, aqueous GB, and aqueous urea−GB. We have computed electrostatic interactions using the particle mesh Ewald method[59] with a direct space cutoff of 1.0 nm and a grid spacing of 0.12 nm. For van der Waals interactions, a 12-6 Lennard-Jones potential with a 1.0 nm cutoff has been used. The pressure of the systems is 1 bar and is held constant by using the Berendsen barostat.[60] We have maintained the geometry of water, urea, and GB molecules during the simulations by using the LINCS algorithm.[61] The temperature of the system is 298 K and it is kept constant by using the velocity rescaling thermostat.[62]

The united atom model has been used for methane. SPCE model is used for water.[63] We have used the OPLS force field for methane and urea.[64−70] The force field parameters of glycine betaine are not defined in the OPLS-AA force field. We have described GB by taking the OPLS-AA force field parameters of similar groups such as $\alpha$-C of GB by using $\alpha$-C of glycine. Because the HF/6-31G** method of Gaussian 09 software package[71] is used for calculating OPLS charges,[72,73] we have used the same for geometry optimization and the calculation of partial charges on GB. The electrostatic potential (ESP) method[74] has been used to drive the partial charges (Table S1 in Supporting Information). A snapshot of GB with atom labels is given in Figure 1.

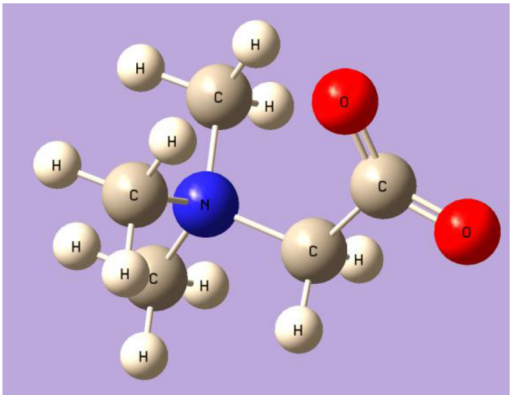


**Figure 1.** Snapshot of glycine betaine with atom labels.

We have computed the density of aqueous GB solutions of different molarities and compared with the experimental values.[75] These values are given in Table 1. There is a fair agreement between these values. The details of the simulation boxes are given in Table 2. System $I_w$ refers to water, system $II_{w\text{-}GB}$ refers to aqueous GB, system $III_{w\text{-}ua}$ refers to aqueous urea, and system $IV_{w\text{-}ua\text{-}GB}$ refers to aqueous urea−GB mixtures. $n_m$, $n_w$, $n_u$,and $n_{GB}$, refer to numbers of methane, water, urea, and GB molecules, respectively (the subscripts referring to methane, water, urea, and GB). In each simulation box, L refers to the length of the box.

**Table 1. Calculated and Experimental Densities of Aqueous GB Solutions of Varying Concentrations**

| concn of aq glycine betaine solutions (M) | calcd densities (g/mL) | exptl densities (g/mL) |
|---|---|---|
| 1 | 1.022 | 1.016 |
| 2 | 1.047 | 1.035 |
| 3 | 1.071 | 1.055 |
| 4 | 1.094 | 1.075 |

**Table 2. Details of the Simulation Boxes Containing Methane, Water, Urea, and GB**

| systems | $n_m$ | $n_w$ | $n_u$ | $n_{GB}$ | $L$ (nm) |
|---|---|---|---|---|---|
| $I_w$ | 50 | 2215 | 0 | 0 | 4.0 |
| $II_{w\text{-}GB}$ | 50 | 1345 | 0 | 160 | 4.0 |
| $III_{w\text{-}ua}$ | 50 | 1466 | 320 | 0 | 4.0 |
| $IV_{w\text{-}ua\text{-}GB}$ | 50 | 593 | 320 | 160 | 4.0 |

Packmole is used to generate the initial configuration of each system.[76] Initially, MD simulations were performed for 50 ns in an *NVT* ensemble for thermal equilibration of each system at a temperature of 298 K. Subsequently, *NPT* simulations for 50 ns were carried out for the equilibration of the pressure of each system by using the Berendsen barostat. Finally, we have generated trajectories of 100 ns for each system using *NPT* MD


DOI: 10.1021/acs.jpcb.5b00556
J. Phys. Chem. B XXXX, XXX, XXX−XXX

simulations by using Parrinello–Rahman pressure coupling.[77,78] In each mixture, we have performed MD simulations at three different temperatures: 278, 298, and 318 K. From these trajectories, we have computed the potentials of mean force (PMFs) between methane molecules with the help of methane–methane pair correlation functions [$g(r)$]. The relation between PMFs and $g(r)$ is

$$W(r) = -kT \ln g(r) \tag{1}$$

We have used a finite temperature difference method to calculate the entropy contributions at each methane–methane separation.[79] Entropy contributions are given by the following formula

$$\Delta S(r) = -\frac{W(r,T+\Delta T) - W(r,T-\Delta T)}{2\Delta T} \tag{2}$$

where $\Delta S(r)$ is the entropy contribution at a methane–methane separation $r$, $W(r,T)$ is the potential of mean force between methane molecules at a methane–methane separation $r$ at temperature $T$, and $\Delta T$ is the temperature difference.

The enthalpy contribution to the potential of mean force is obtained from

$$\Delta H(r) = W(r) + T\Delta S(r) \tag{3}$$

## 3. RESULTS

We first present our results on PMFs and equilibrium constants (sections 3.1 and 3.2) at room temperature. The temperature dependence of PMFs and the decomposition of PMF($r$) into enthalpy and entropy are given in section 3.3. This is followed by solvation free energies of methane in different systems (section 3.4), solvation structures and preferential solvation of methane molecules in the aqueous solutions of urea and GB (section 3.5), diffusional behavior of water molecules in the four systems (section 3.6), and hydrogen-bonding properties of water in the four systems (section 3.7).

**3.1. Methane–Methane Potentials of Mean Force in the Presence of Osmolytes.** We have shown the potential of mean force between methane molecules in water (black curve), aqueous GB (red curve), aqueous urea (blue curve), and aqueous urea–GB mixtures (magenta curve) in Figure 2.

In Figure 2, there are three minima in curves $I_w$, $II_{w\text{-}GB}$, and $III_{w\text{-}ua}$ whereas curve $IV_{w\text{-}ua\text{-}GB}$ shows two minima. The first minimum corresponds to a contact minimum (CM) and subsequent minima correspond to solvent-separated minima (SSM). In the third minimum, more than one solvent molecule may be inserted between the methane molecules. The contact minimum represents hydrophobic association and solvent-separated minima represent the hydrophobic solvation of methane molecules in these mixtures. The differences between PMFs obtained from two sets of 50 ns simulations are less than 0.5 kJ mol$^{-1}$ (Figure S1, given in Supporting Information).

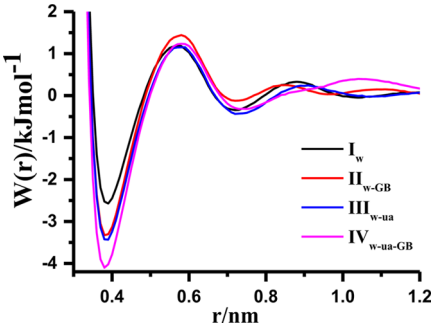


**Figure 2.** Potentials of mean force (PMFs) between methane molecules in $I_w$ (black curve), $II_{w\text{-}GB}$ (red curve), $III_{w\text{-}ua}$ (blue curve), and $IV_{w\text{-}ua\text{-}GB}$ mixtures (magenta curve).

The positions and free energies of contact minima, first transition states and first solvent-separated minima (second minima), and first transition state barriers with respect to CM and with respect to SSM in water, aqueous GB, aqueous urea and aqueous urea–GB mixtures are given in Table S2 (Supporting Information).

As we go from water to aqueous GB solution, the depth of contact minimum changes from −2.6 to −3.3 (all energy values in kJ mol$^{-1}$) and the height of transition state barrier with respect to contact minimum changes from 3.8 to 4.7. The depth of solvent-separated minimum changes from −0.3 to −0.1. From these differences, we note that hydrophobic association of methane increases and hydrophobic solvation marginally decreases on the addition of GB to water. As we go from water to aqueous urea mixture, the depth of CM changes from −2.6 to −3.4 kJ mol$^{-1}$ and the height of transition state barrier with respect to CM changes from 3.8 to 4.6 kJ mol$^{-1}$. The depth of SSM changes from −0.3 to −0.4 kJ mol$^{-1}$. The hydrophobic association of methane molecules is enhanced on the addition of urea into water and the effect on hydrophobic solvation is marginal. As we add glycine betaine (GB) into aqueous urea, the depth of contact minimum increases from −3.4 to −4.0 kJ mol$^{-1}$. The depth of SSM is not affected. The height of the transition state barrier with respect to the contact minimum increases from 4.6 to 5.3 kJ mol$^{-1}$. The hydrophobic association of methane molecules is enhanced. Though hydrophobic association is enhanced in all cases, the effect on hydrophobic solvation is marginal when one considers only the barrier heights for solvation. The barrier heights for solvation in all the cases are 1.5 ± 0.1 kJ mol$^{-1}$.

**3.2. Equilibrium Constants.** We have calculated the equilibrium constants for methane molecules in water, aqueous GB, aqueous urea, and aqueous urea–GB solutions. The equilibrium constant is defined as

$$[\mathrm{CM}] = 4\pi \int_0^{r_1} r^2 e^{-W(r)/k_B T}\, dr \tag{4}$$

$$[\mathrm{SSM}] = 4\pi \int_{r_1}^{r_2} r^2 e^{-W(r)/k_B T}\, dr \tag{5}$$

$$K_{eq} = \frac{[\mathrm{SSM}]}{[\mathrm{CM}]} \tag{6}$$

where $K_{eq}$ is the equilibrium constant, [SSM] is the area (nm$^3$) under the curve between $r_1$ (for TS1 = 0.59 nm) and $r_2$ (for TS2 = 0.88 nm), [CM] is calculated as the area (nm$^3$) under the curve up to $r_1$ (for TS1 = 0.59 nm), $W(r)$ is the PMF of methane molecules, $k_B$ is the Boltzman's constant, $T$ is the temperature of the system, $r_1$ is the position of the first maximum, and $r_2$ is the position of second maximum in the corresponding PMF curve. The equilibrium constants for methane molecules in these mixtures are given in Table 3.

It is seen from Table 3 that the association of methane increases as we go from water to aqueous GB, water to aqueous urea, and water to aqueous urea–GB. The association in the presence of both osmolytes seems to be the cumulative effect of the individual osmolytes. As we add GB to the aqueous urea



DOI: 10.1021/acs.jpcb.5b00556
J. Phys. Chem. B XXXX, XXX, XXX–XXX

**Table 3. Equilibrium Constants for Methane Molecules in $I_w$, $II_{w\text{-}GB}$, $III_{w\text{-}ua}$, and $IV_{w\text{-}ua\text{-}GB}$ Mixtures[a]**

| systems | [CM] ($nm^3$) | [SSM] ($nm^3$) | equilibrium constants ([SSM]/[CM]) |
|---|---|---|---|
| $I_w$ | 0.83 | 1.97 | 2.37 |
| $II_{w\text{-}GB}$ | 0.98 | 1.82 | 1.86 |
| $III_{w\text{-}ua}$ | 1.05 | 2.02 | 1.92 |
| $IV_{w\text{-}ua\text{-}GB}$ | 1.22 | 1.98 | 1.62 |

[a][CM] is calculated as the area of eq 4 under the curve up to $r_1$ (for TS1 = 0.59 nm). [SSM] is the area of eq 5 under the curve between $r_1$ (for TS1 = 0.59 nm) and $r_2$ (for TS2 = 0.88 nm).

mixture, the equilibrium constant changes from 2.37 to 1.62. If [SSM] is taken to be a measure of solvation, then the two osmolytes have an opposing effect. When both urea and GB are added, they seem to cancel each other's effect. Although this interpretation is sensitive to the value of $r_2$ chosen for the upper limit of integration, the same trend is observed for other values of $r_2$. The equilibrium constants, defined as [SSM]/[CM] decrease as we go from only water to water−urea and to water−GB. When both osmolytes are added, the decrease in equilibrium constants is more than the decrease in individual cases.

**3.3. Thermodynamics of Hydrophobic Association and Solvation of Methane Molecules.** We have used a finite temperature difference method to calculate the entropy contributions at each methane−methane separation. We have computed the thermodynamic quantities ($\Delta G$, $-T\Delta S$, and $\Delta H$, all in kJ $mol^{-1}$) as a function of methane−methane distance by using eqs 2 and 3. The potentials of mean force of methane molecules in water ($I_w$) (A), aqueous GB ($II_{w\text{-}GB}$) (B), aqueous urea ($III_{w\text{-}ua}$) (C), and aqueous urea−GB ($IV_{w\text{-}ua\text{-}GB}$) (D) solutions at three temperatures: 278, 298, and 318 K are given in Figure S2 (Supporting Information). On increasing the temperature, the depth of CM increases in all these mixtures.

The thermodynamic quantities ($\Delta G$, $-T\Delta S$, and $\Delta H$) for the hydrophobic association and hydrophobic solvation of methane molecules as a function of methane−methane distance for the four solutions are given in Figure 3.

In A, B, C, and D of Figure 3 above, the black curve represents the potential of mean force ($\Delta G$) between methane molecules, the red curve represents entropy contribution ($-T\Delta S$) to the PMFs and the blue curve represents the enthalpy contribution ($\Delta H$) to the PMFs.

In water, the association between methane molecules is stabilized by entropy and the hydrophobic solvation is destabilized by entropy. Local minima in enthalpy (relative to the transition state, which is destabilized) also contribute favorably to both association and solvation of methane.

In aqueous GB mixture, when we are approaching the contact minimum from the transition state, the CM is stabilized by entropy and favored by enthalpy. On the contrary, the solvent-separated minimum is favored by enthalpy and destabilized by entropy. The magnitude of enthalpy stabilization of SSM is less than in water.

In the aqueous urea mixture, as we move from transition state to contact minimum, the association of methane is stabilized by entropy and disfavored by enthalpy. The magnitudes of stabilization and destabilization are different from that in water and aqueous GB.

In aqueous urea−GB mixture, the hydrophobic association as well as hydrophobic solvation of methane molecules are stabilized by entropy and favored by enthalpy.

**3.4. Solvation Gibbs Free Energies of Methane in Water, Aqueous GB, Aqueous Urea, and Aqueous Urea−GB Mixtures.** Ben-Naim[80] has used Widom's potential distribution theorem[81] to define the solvation free energy of a solute. The solute solvent binding interaction $B_s$ is established by inserting a test particle S at a random point in an $N$-particle liquid configuration. It is the difference of the $N + 1$ and $N$ particle potential energies, $B_s = U_{N+1} - U_N$. The standard Gibbs free energy change ($\Delta G^*$) is calculated as follows.

$$\Delta G^* = -RT \ln[\langle V \exp(-B_s/RT)\rangle_{NPT}/\langle V\rangle_{NPT}] \quad (7)$$

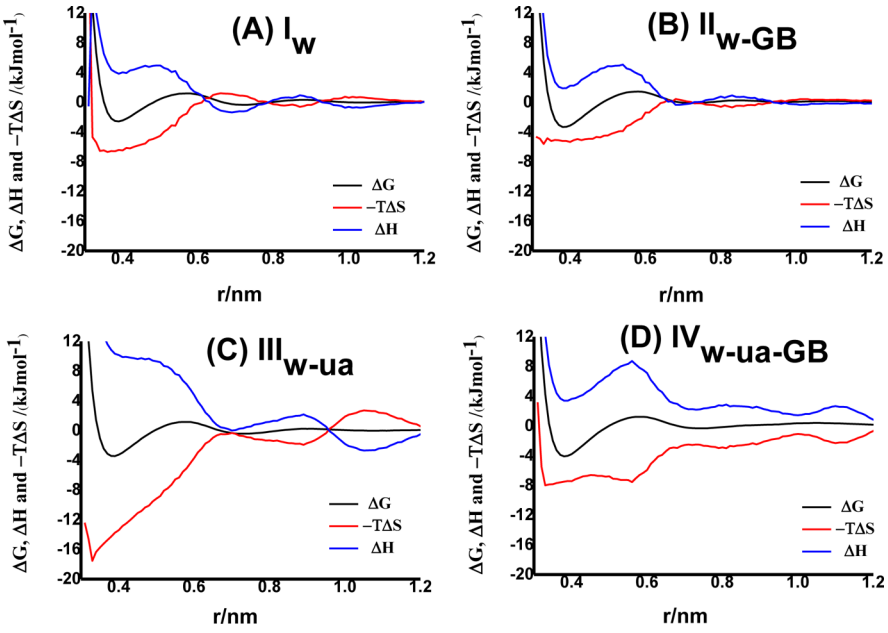


**Figure 3.** Thermodynamic quantities ($\Delta G$, $-T\Delta S$, and $\Delta H$) for the hydrophobic association of methane molecules in $I_w$ (A), $II_{w\text{-}GB}$ (B), $III_{w\text{-}ua}$ (C), and $IV_{w\text{-}ua\text{-}GB}$ (D) solutions.



DOI: 10.1021/acs.jpcb.5b00556
J. Phys. Chem. B XXXX, XXX, XXX−XXX

Table 4. Solvation Free Energies of Methane in $I_w$, $II_{w\text{-}GB}$, $III_{w\text{-}ua}$, and $IV_{w\text{-}ua\text{-}GB}$ at Three Temperatures 278, 298, and 318 K

| | $\Delta G$ (kJ mol$^{-1}$) | | | | |
|---|---|---|---|---|---|
| mixtures | 278 K | 298 K | 318 K | $\Delta H$ (298 K) (kJ mol$^{-1}$) | $-T\Delta S$ (298 K) (kJ mol$^{-1}$) |
| $I_w$ | 9.8(±0.1) | 9.2(±0.1) | 8.3(±0.1) | −2.0 | 11.2 |
| $II_{w\text{-}GB}$ | 11.2(±0.1) | 10.2(±0.1) | 9.1(±0.1) | −5.4 | 15.6 |
| $III_{w\text{-}ua}$ | 10.9(±0.1) | 9.7(±0.1) | 8.6(±0.2) | −7.4 | 17.2 |
| $IV_{w\text{-}ua\text{-}GB}$ | 14.8(±0.2) | 11.5(±0.1) | 10.0(±0.1) | −24.3 | 35.8 |

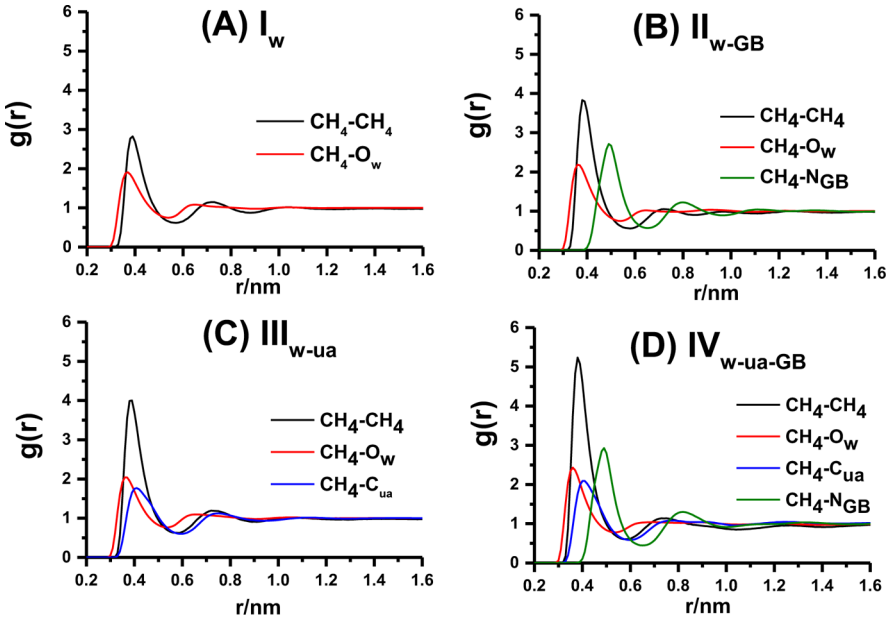


**Figure 4.** Radial distribution functions of methane with methane, water, urea, and GB molecules in $I_w$ (A), $II_{w\text{-}GB}$ (B), $III_{w\text{-}ua}$ (C), and $IV_{w\text{-}ua\text{-}GB}$ solutions (D).

Here, the ensemble average is taken over solvent configurations at constant pressure $P$ and temperature $T$. In eq 7, $V$ denotes the system volume and $\langle V\rangle_{NPT}$ its ensemble average at constant $P$ and $T$.

The solvation free energies of methane in water ($I_w$), aqueous GB ($II_{w\text{-}GB}$), aqueous urea ($III_{w\text{-}ua}$), and aqueous urea–GB ($IV_{w\text{-}ua\text{-}GB}$) at three temperatures 278, 298, and 318 K are given in Table 4.

At room temperature, the solvation free energies of methane are 9.2, 10.2, 9.7, and 11.5 kJ mol$^{-1}$ in water, water–GB, water–urea, and water–urea–GB mixtures, respectively. These results suggest that methane is less soluble in the mixtures of osmolytes than in water. The solubility of methane in these mixtures is favored by enthalpy and disfavored by entropy. In the presence of osmolytes, hydrophobic association of methane is enhanced, which is supported by solvation free energies.

**3.5. Solvation Structures and Preferential Solvation of Methane Molecules in the Aqueous Solutions of Urea and GB.** *3.5.1. Radial Distribution Functions.* The radial distribution functions (RDFs or $g(r)$'s) of methane with methane, urea, and GB molecules in water (A), aqueous GB (B), aqueous urea (C), and aqueous urea–GB (D) solutions are given in Figure 4. The RDFs between $CH_4$–$CH_4$, $CH_4$–$O_w$, $CH_4$–$N_{GB}$, and $CH_4$–$C_{ua}$ are represented by black, red, green, and blue curves, respectively.

We have obtained the RDFs of methane with each site of GB in the water–GB mixture (Figure S3, Supporting Information). We observed that the interaction of methane with the nitrogen site of GB is stronger in comparison to other sites of GB. The RDFs of methane with methane and the oxygen site of water are shown in Figure 4A. In water, the interaction of methane with methane is more favorable than the methane–water interaction. In the water–GB mixture (Figure 4B), the methane–methane interaction is stronger than the methane–water and methane–GB interactions. We have also obtained the RDFs of methane with each site of urea in the water–urea mixture (Figure S4, Supporting Information). We observed that the interaction of methane with the carbon site of urea is stronger in comparison to other sites of urea. In the water–urea mixture (Figure 4C), the methane–methane interaction is stronger than the methane–water and methane–urea interactions. The interaction of methane with water is enhanced in the water–urea–GB mixture (Figure 4D). The local density of methane around methane is enhanced in the presence of both urea and GB (Figure 4D).

To examine the hydration of methane, it is important to study the effect of urea and glycine betaine on the water structure. Therefore, we have reported the RDFs of water with water molecules in water (black line), water–GB (red line), water–urea (blue line), and water–urea–GB (magenta line) solutions in Figure 5. The locations of the first peak and the second peak are at 2.8 and 4.5 Å, respectively. The first peak represents the hydrogen-bonded first neighbor and the second peak represents the tetrahedrally located second neighbor. As we go from water to aqueous GB, the first peak height of $O_w$–$O_w$ RDFs increases from 2.9 to 4.1, which suggests that the water–water interaction is enhanced. The peak height is 3.6 in the water–urea solution, which suggests that urea also


DOI: 10.1021/acs.jpcb.5b00556
J. Phys. Chem. B XXXX, XXX, XXX–XXX

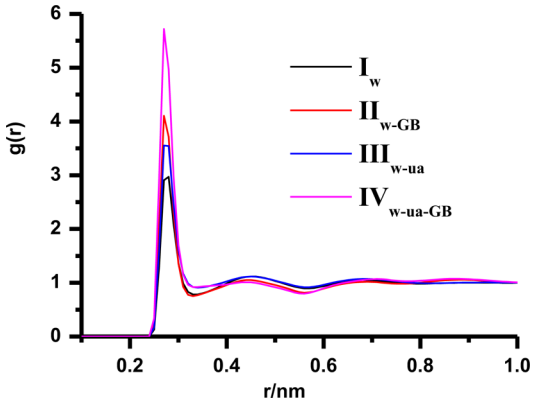


**Figure 5.** Radial distribution functions of water with water molecules in $I_w$ (black curve), $II_{w\text{-}GB}$ (red curve), $III_{w\text{-}ua}$ (blue curve), and $IV_{w\text{-}ua\text{-}GB}$ (magenta curve) solutions.

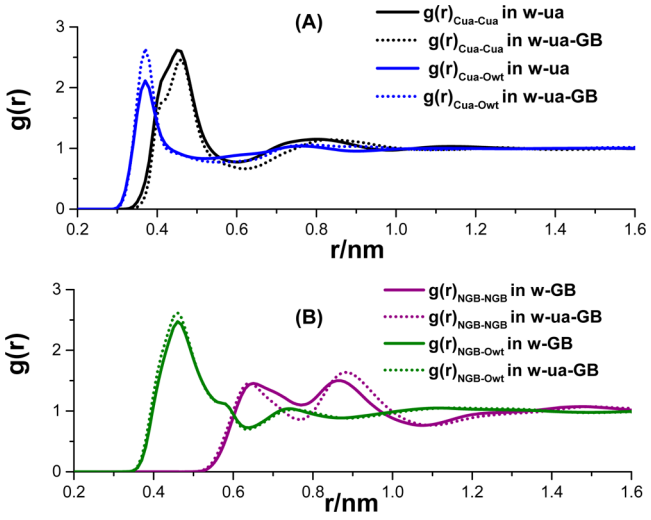


**Figure 6.** Radial distribution functions between urea−urea (solid black) in $III_{w\text{-}ua}$, urea−urea (dotted black) in $IV_{w\text{-}ua\text{-}GB}$, urea−water (solid blue) in $III_{w\text{-}ua}$, and urea−water (dotted blue) in $IV_{w\text{-}ua\text{-}GB}$ (A). Radial distribution functions between GB−GB (solid purple) in $II_{w\text{-}GB}$, GB−GB (dotted purple) in $IV_{w\text{-}ua\text{-}GB}$, GB−water (solid green) in $II_{w\text{-}GB}$, and GB−water (dotted green) in $IV_{w\text{-}ua\text{-}GB}$ (B).

strengthens the water−water interaction. The first peak height of the $O_w$−$O_w$ radial distribution function is 5.7 in the aqueous urea−GB mixture. In the $O_w$−$O_w$ RDF, the first valley becomes broader and the second peak becomes less pronounced in the presence of urea. These are the evidence for the collapse of the second shell of water around water in the presence of urea.[82] GB tends to deepen the first valley of the $O_w$−$O_w$ RDF and the second peak becomes more pronounced. On the addition of GB in aqueous urea mixture, the water−water interaction and urea−water interaction are enhanced (Table 5).

The RDFs between the sites of cosolvents and cosolvents and solvents are shown in Figure 6. The RDFs between urea−urea in aqueous urea (solid black) and in aqueous urea−GB (dotted black) and between urea−water in aqueous urea (solid blue) and in aqueous urea−GB (dotted blue) are shown in Figure 6A. The RDFs between GB−GB in aqueous GB (solid purple) and in aqueous urea−GB (dotted purple) and between GB−water in aqueous GB (solid green) and in aqueous urea−GB (dotted green) are shown in Figure 6B. On addition of GB into the water−urea solution, the local density of water around urea is enhanced. Therefore, urea molecules are excluded from the methane surface. As we add urea into the water−GB mixture, the interactions between GB and water molecules are enhanced (Figure S5 of Supporting Information). Hence, methane molecules are not preferentially solvated by GB.

The first peak heights of radial distribution functions of methane−methane, methane−water, methane−GB, methane−urea, water−water, urea−urea, and urea−water in water, water−GB, water−urea, and water−urea−GB mixtures are given in Table 5.

The first peak height of methane−GB RDF is 2.9 (system $IV_{w\text{-}ua\text{-}GB}$) and methane−urea RDF is 2.1 (system $IV_{w\text{-}ua\text{-}GB}$) which suggests preferential solvation of methane by GB over urea. The first peak heights of $O_{GB}$-$O_{wt}$ RDF (Figure S5, Supporting Information) are 3.7 (water−GB mixture) and 4.8 (water−urea−GB mixture), indicating that as we go from aqueous GB to the aqueous urea−GB mixture, the GB−water interaction is enhanced.

The computed values of running coordination numbers of water, urea, and GB molecules in the first coordination shell of methane described in the next section also support these findings.

*3.5.2. Running Coordination Numbers (RCNs) of Water, Urea, and GB Molecules around Methane Molecules.* The running coordination numbers are defined as

$$n_{\alpha\beta} = 4\pi\rho_\beta \int_{r_1}^{r_2} r^2 g_{\alpha\beta}(r)\, dr \tag{8}$$

where $n_{\alpha\beta}$ represents the number of atoms of type $\beta$ surrounding type $\alpha$ in a shell extending from $r_1$ to $r_2$ and $\rho_\beta$ is the number density of $\beta$ type species in the system. For the calculation of the first solvation shell coordination number, the value of $r_1$ is zero and the value of $r_2$ is the first minimum in the radial distribution function.

The running coordination numbers of water, urea, and GB in the first coordination shell of methane in water, aqueous GB, aqueous urea, and aqueous urea−GB mixtures are given in Table 6.

In water−GB mixture, the value $N_w/N_{GB}$ is 8.5 in the first coordination shell of methane and 8.4 in the bulk, which suggests that methane has a marginal preference for water molecules. In $III_{w\text{-}ua}$, the value of $N_w/N_{ua}$ is 5.0 in the first coordination shell of methane and 4.5 in the bulk, which

**Table 5. First Peak Heights of Radial Distribution Functions of Methane−Methane, Methane−Water, Methane−GB, Methane−Urea, Water−Water, Urea−Urea, and Urea−Water in $I_w$, $II_{w\text{-}GB}$, $III_{w\text{-}ua}$, and $IV_{w\text{-}ua\text{-}GB}$ Mixtures**

| systems | $CH_4$−$CH_4$ | $CH_4$−$O_W$ | $CH_4$−$N_{GB}$ | $CH_4$−$C_{ua}$ | $O_w$−$O_w$ | $C_{ua}$−$C_{ua}$ | $C_{ua}$−$O_w$ |
|---|---|---|---|---|---|---|---|
| $I_w$ | 2.8 | 1.9 | | | 2.9 | | |
| $II_{w\text{-}GB}$ | 3.8 | 2.2 | 2.7 | | 4.1 | | |
| $III_{w\text{-}ua}$ | 4.0 | 2.0 | | 1.8 | 3.6 | 2.6 | 2.1 |
| $IV_{w\text{-}ua\text{-}GB}$ | 5.2 | 2.4 | 2.9 | 2.1 | 5.7 | 2.4 | 2.6 |



DOI: 10.1021/acs.jpcb.5b00556
J. Phys. Chem. B XXXX, XXX, XXX−XXX

**Table 6. Running Coordination Numbers in the First Coordination Shell of Methane in the Presence of Osmolytes[a]**

| systems | $N_w$ | $N_{GB}$ | $N_{ua}$ | $N_w/N_{ua}$ | $N_w/N_{GB}$ | $N_{ua}/N_{GB}$ |
|---|---|---|---|---|---|---|
| $I_w$ | 25.9 | | | | | |
| $II_{w\text{-}GB}$ | 22.8 | 2.7 | | | 8.5 (**8.4**) | |
| $III_{w\text{-}ua}$ | 16.9 | | 3.4 | 5.0 (**4.5**) | | |
| $IV_{w\text{-}ua\text{-}GB}$ | 10.4 | 2.7 | 4.8 | 2.2 (**1.8**) | 3.9 (**3.7**) | 1.8 (**2.0**) |

[a] $N_w$, $N_{GB}$, and $N_{ua}$ represent the number of water, GB, and urea molecules, respectively. Values in parentheses are for bulk. The cut-off for the first coordination shell of methane is 0.66 nm for all the mixtures.

suggests that methane is preferentially solvated by water molecules.

In the aqueous urea−GB mixture, the $N_w/N_{GB}$ ratio is 3.9 in the first coordination shell of methane and 3.7 in the bulk. The $N_w/N_{ua}$ ratio is 2.2 in the first coordination shell of methane and 1.8 in the bulk. These results also indicate that methane is preferentially solvated by water over GB and urea. The value of $N_{ua}/N_{GB}$ is 1.8 in the first coordination shell of methane and 2.0 in the bulk, indicating a marginal, but significant, domination of GB over urea in the first coordination shell. The running coordination numbers of water molecules in the first coordination shell of urea/GB (Table S3, Supporting Information) suggest that the GB−water interaction is stronger than the urea−water interaction.

*3.5.3. Preferential Binding of Methane with Urea and GB.* To investigate the preferential solvation of methane in these systems, we calculate the excess coordination numbers of water, urea, and GB molecules around methane. The excess coordination number is defined as[53,83]

$$N_{\alpha\beta}(r_c) = 4\pi\rho_\beta \int_0^{r_c} r^2[g_{\alpha\beta}(r) - 1]\, dr \quad (9)$$

Here $4\pi\rho_\beta r^2 g_{\alpha\beta}(r)$ is the average number of $\beta$ molecules around an $\alpha$ molecule in a spherical shell of width d$r$ at radius $r$ and $4\pi\rho_\beta r^2$ d$r$ is the average number of $\beta$ molecules in that spherical shell that are uninfluenced by $\alpha$ (as in a uniformly random distribution). Therefore, $N_{\alpha\beta}(r_c)$ represents the excess number of $\alpha$ molecules around a $\beta$ molecule measured up to $r = r_c$. The excess coordination numbers (ECNs) of water, urea, and GB molecules around methane in four solutions are given in Figure S6 (Supporting Information). The KB theory gives relations between integrals of radial distribution functions and properties of solutions. The Kirkwood−Buff integral between species $i$ and $j$ is defined as[83]

$$G_{ij}(r) = 4\pi \int_0^r [g_{ij}(r') - 1] r'^2\, dr' \quad (10)$$

The relation between preferential binding parameter ($\nu$) and KB integrals for methane in the mixture of solvent and cosolvent is given by[84]

$$\nu = \rho_3(G_{23} - G_{21}) \quad (11)$$

Here, $G_{23}$ (when $r$ in eq 10 is $\infty$) is the KB integral between the solute (2, methane) and cosolvent (3, urea or GB), $G_{21}$ (when $r$ in eq 10 is $\infty$) is the KB integral between the solute (2) and solvent (1, water), and $\rho_3$ is the number density of the cosolvent (urea or GB) in the mixtures. The positive value of $\nu$ indicates preferential binding of solute with cosolvent whereas negative values favor solvent, i.e., water. We have calculated preferential binding parameters ($\nu$) for methane in aqueous GB and aqueous urea. The preferential binding constants of methane with GB in the water−GB mixture and with urea in the water−urea mixture are given in Table 7. The preferential

**Table 7. Preferential Binding Constants ($\nu$) of Methane with GB in $II_{w\text{-}GB}$ and with Urea in $III_{w\text{-}ua}$**

| systems | $\nu$ |
|---|---|
| $II_{w\text{-}GB}$ | −0.05 |
| $III_{w\text{-}ua}$ | −1.19 |

binding parameters for methane with each methyl site of GB in water−urea−GB solutions are given in Table S4 (Supporting Information). All values are negative, which suggest that there is no preferential binding of methane with methyl sites of GB.

The negative values of preferential binding constants ($\nu$) support a strong preference for water, especially in water urea solutions. The local correlations between solution components and salting-out thermodynamics can be adequately explained by calculating the quantity $G_{21}(r) - G_{23}(r)$ obtained using the above equation based on Kirkwood−Buff theory (also known as fluctuation theory of solutions). The theory relates integral over molecular distribution functions to particle number fluctuations. These are given in Figure 7. For all the systems,

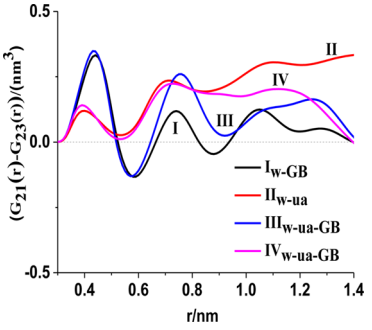


**Figure 7.** Running KBIs $G_{ij}(r)$ between methane−water ($G_{21}(r)$) minus methane−cosolvent ($G_{23}(r)$) in aqueous GB, aqueous urea, and aqueous urea−GB solutions. Subscript 1 refers to water, 2 refers to methane, and 3 refers to urea (magenta curve) and GB (blue curve).

we observe large ranges of distances where $(G_{21}(r) - G_{23}(r)) > 0$ (oscillating due to structural fluctuations). The negative fluctuations in the small range between 0.5 and 0.7 nm in systems with GB molecules are due to the larger size of GB molecules in the first solvation shell of methane. Beyond 0.7 nm the value is largely positive, suggesting the preferential hydration and salting-out of methane by water. The Kirkwood−Buff integrals ($G_{ij}$) in the simulations do not asymptotically go to zero if there are local solvent fluctuations around a species of interest, leading to preferential solvation. In Figure 7, $I_{w\text{-}ua}$ does not go to zero at half box length because $G_{21} - G_{23}$ has an asymptotic value of 0.30 ± 0.03. In the distance range from 1.4 to 2.0 nm, the values of $G_{21} - G_{23}$ fluctuate marginally because the asymptotic values of pair distribution functions do not exactly become one in simulations beyond 1.4 nm. Considerable effort by several workers has been made to understand the microheterogeneous nature of aqueous solutions as well as the asymptotic values of $G_{ij}$ at large $r$.[54,85−87] These studies support our conclusions.

**3.6. Diffusional Behavior of Water Molecules in the Systems $I_w$, $II_{w\text{-}GB}$, $III_{w\text{-}ua}$, and $IV_{w\text{-}ua\text{-}GB}$.** The diffusion


DOI: 10.1021/acs.jpcb.5b00556
J. Phys. Chem. B XXXX, XXX, XXX−XXX

coefficients ($D$) are calculated from the mean square displacements, using Einstein's relation,

$$D = \frac{\langle |r_i(t + \Delta t) - r_i(t)|^2 \rangle}{6t} \quad (12)$$

where $r_i(t)$ is the position of the $i$th water molecule at time $t$.

We have studied the diffusional pattern of water molecules in these mixtures. It is observed that urea and GB both tend to decrease the diffusion of water molecules. The diffusion coefficients of water molecules in the four mixtures are given in Table 8. The values of diffusion coefficients are 2.28, 0.40, 1.45, and 0.06 ($10^{-5}$ cm$^2$ s$^{-1}$) in water, water−GB, water−urea, and water−urea−GB mixtures, respectively, which are found to be in reasonable agreement with available reported values.[47,88] The diffusion of water molecules is less in the mixtures of these osmolytes, suggesting that they strengthen the water−water interaction. The lower values of $D$ in water−GB and water−urea−GB suggest strong association of GB with water molecules (Figure S5, Supporting Information).

**Table 8. Diffusion Coefficients ($10^{-5}$ cm$^2$ s$^{-1}$) of Water Molecules in $I_w$, $II_{w\text{-}GB}$, $III_{w\text{-}ua}$, and $IV_{w\text{-}ua\text{-}GB}$**

| systems | diffusion coeff |
|---|---|
| $I_w$ | 2.28 |
| $II_{w\text{-}GB}$ | 0.40 |
| $III_{w\text{-}ua}$ | 1.45 |
| $IV_{w\text{-}ua\text{-}GB}$ | 0.06 |

**3.7. Hydrogen-Bonding Properties of Water−Urea−GB Solutions.** Hydrogen bonds in this study are characterized by the H-acceptor distances that are less than 0.26 nm and the acceptor-H-donor angles greater than 130°. We have calculated the lifetimes of hydrogen bonds of water molecule in the mixtures of osmolytes. The computation of lifetimes of hydrogen bonds follows the work of Chandler et al.[89] The fluctuation in hydrogen bond populations is characterized by the following correlation functions $c(t)$.

$$c(t) = \langle h(0)\, h(t) \rangle / \langle h \rangle \quad (13)$$

Here, $h(t)$ is the hydrogen bond population operator. The value of the operator is 1 when two water molecules are hydrogen bonded and zero otherwise. $c(t)$ is the probability that the hydrogen bond is intact between two water molecules at time $t$, given that the both waters are hydrogen bonded at time zero. The rate of relaxation to equilibrium is given by

$$k(t) = -\mathrm{d}c/\mathrm{d}t = -\langle \dot{h}(0)[1 - h(t)] \rangle / \langle h \rangle \quad (14)$$

where $-k(t)$ is the average rate of change of hydrogen-bond population, $\dot{h}(0) = (\mathrm{d}h/\mathrm{d}t)_{t=0}$ (because $\langle h(0)\, \dot{h}(t) \rangle = -\langle \dot{h}(0)\, h(t) \rangle$ and $\langle \dot{h}(0) \rangle = 0$).

The functions $c(t)$ and $k(t)$ will decay exponentially only if the lifetime distribution is exponential. The nonexponential relaxation of hydrogen bonding is because of the coupling between hydrogen bond population and diffusion. Two hydrogen-bonded molecules can diffuse far away if the hydrogen bond between them breaks and a broken hydrogen bond can re-form if a molecule reverses its direction and diffuses back to its hydrogen-bonded partner.

The probabilities $c(t)$ and $n(t)$ correspond to local population that can interconvert. Hence, the overall hydrogen bond kinetics is given by

$$\mathrm{d}c/\mathrm{d}t = -kc(t) + k'n(t) \quad (15)$$

where $k$ and $k'$ are respective rate constants for the breaking and making of hydrogen bonds between a near-neighbor pair of water molecules, $n(t)$ is $n(t) = \int_0^t \mathrm{d}t'\, k_{in}(t')$ and $k_{in}(t) = -\langle \dot{h}(0)[1 - h(t)]H(t) \rangle / \langle h \rangle$. The physical meaning of $1/k$ is that of the average hydrogen-bond lifetime. $H(t)$ is unity if the oxygen−oxygen distance of two water molecules is less than 3.5 Å. The computed values of number of hydrogen bonds in the four mixtures are given in Table 9.

**Table 9. Number of Hydrogen Bonds Per Water Molecule in the Bulk in $I_w$, $II_{w\text{-}GB}$, $III_{w\text{-}ua}$, and $IV_{w\text{-}ua\text{-}GB}$**

| | HB per water molecule in the bulk | | |
|---|---|---|---|
| systems | 278 K | 298 K | 318 K |
| $I_w$ | 3.82 | 3.75 | 3.68 |
| $II_{w\text{-}GB}$ | 2.87 | 2.86 | 2.82 |
| $III_{w\text{-}ua}$ | 3.07 | 2.96 | 2.89 |
| $IV_{w\text{-}ua\text{-}GB}$ | 1.66 | 1.62 | 1.59 |

As we go from water to the mixtures of osmolytes, the number of hydrogen bonds per water molecule decreases but the lifetimes of hydrogen bonds increase (Table S5, Supporting Information) due to the strong association of water with osmolytes. There is a gradual decrease with temperature, as expected. The hydrogen bond time correlation functions ($c(t)$) are given in Figure S7 (Supporting Information). In the mixtures of osmolytes, slower relaxations of $c(t)$ have been observed in comparison to water. These calculations suggest that there is strong hydrogen bonding between water molecules in the mixture of osmolytes.

## 4. DISCUSSIONS

**4.1. Neat Water.** The PMF curve (Figure 2) shows hydrophobic association of methane in neat water. The appearance of a contact minimum at 0.39 nm suggests the existence of methane clusters/association. The curve also shows the existence of solvent-separated minimum at 0.72 nm corresponding to hydrophobic solvation of methane molecules. The two states are separated by a low barrier of 1.2 kJ mol$^{-1}$. The clustering of methane (the phenomenon of hydrophobic association) has been reported earlier.[54]

The contact minimum is stabilized by entropy and favored by enthalpy. When methane molecules approach the contact minima, hydrogen bonds between water molecules are broken.[87] When the CM is approached from the transition state, the entropy contribution monotonically increases (i.e., $-T\Delta S$ becomes more negative), whereas the enthalpy contribution initially increases and finally reaches a local minimum at the CM (Figure 3). The solvent-separated minimum is favored by enthalpy and disfavored by entropy. At SSM, more hydrogen bonds are formed because of cage like structure of water molecules around methane.[90] The transition state barrier (between CM and first SSM) is stabilized by entropy and opposed by enthalpy because hydrogen bonds are broken.

The equilibrium constant calculated for methane molecules in neat water (Table 3) suggests a relatively sustainable hydrophobic association.

At the temperature at which simulations have been carried out, the tendency of water to maintain intersolvent hydrogen bonding prevails. The calculation of diffusion constants (Table



DOI: 10.1021/acs.jpcb.5b00556
J. Phys. Chem. B XXXX, XXX, XXX−XXX

8) and the number of hydrogen bonds per water molecule (Table 9) illustrate this fact. This tendency creates a low entropy hydrogen-bonded fence[91] surrounding methanes (nonpolar solutes), facilitating the hydrophobic solvation of methane. The process of "cavity formation" occurs. The flexibility of the medium with regard to spontaneous opening of suitable cavities is determined by entropic opposition to solvation. On the basis of RDFs of methane with methane and oxygen site of water shown in Figure 4A, it can be inferred that, in water, interaction of methane with methane is more favorable than the methane−water interaction. The inference is supported by the excess coordination numbers obtained for water around methane (Figure S6, Supporting Information).

**4.2. Water−GB.** The addition of GB to water shows enhanced hydrophobic association of methane in aqueous GB. Although the depths of CM and SSM change, their locations are not altered. The two states are separated by an energy barrier of 1.4 kJ $mol^{-1}$ (Figure 2).

The contact minimum is dominated by entropy and favored by enthalpy, because, when methane molecules approach the contact minima, there is a removal of water and GB molecules from the coordination shell of methane. When the CM is approached from the transition state, the entropy contribution monotonically increases, whereas the enthalpy contribution initially increases and finally reaches a local minimum at the CM. The solvent-separated minimum is favored by enthalpy and marginally disfavored by entropy. At SSM, enthalpy and entropy contributions are very close to each other. We note that the oscillations in $\Delta H$ and $T\Delta S$ in the water−GB mixture, beyond SSM, are reduced significantly compared to those in the water−urea mixture as well as in pure water. The size of GB as well as the strongly associated structures in water and water−urea are responsible for this.

In water−GB mixture, methane prefers methane over water. The analysis of RDFs by KB integrals suggests preferential solvation of methane by water. Effects of addition of protecting osmolytes such as TMAO on hydrophobic interactions of methane have been reported earlier.[57] It is worth mentioning that both TMAO and GB belong to the same class of osmolytes. Paul and co-workers[57] have suggested in their work on TMAO osmolyte that the hydrophobic methane molecules are compatible with the methyl groups of TMAO and can substitute methyl groups in TMAO molecules. There are differences in the effect of these two osmolytes on preferential solvation of methane molecules. There is a negligible effect of TMAO on the hydrophobic association of methane[57] whereas GB enhances the hydrophobic association of methane, i.e., salting-out of methane. The preferential solvation of methane by water over GB is supported by the RCN values. The preferential binding constants ($\nu$ strongly in favor of GB) for methane in aqueous GB further support this observation. The analysis of RDFs by KB integrals also indicates the preferential solvation by water (Figure 7). The strong association between water and GB (Figure S5 and Table S3, Supporting Information) is also responsible for the exclusion of GB from methane surface.

The hydrophobic association between methane molecules is expected to be more because of preferential methane-water interaction over GB. The value of the equilibrium constant obtained indicates enhanced association of methane molecules.

The two synergistic effects in aqueous GB, namely, an increase in hydrophobic association due to preferential methane-water interaction in the presence of GB and methane-methyl group compatibility causes "salting out" of methane molecules in the mixture.

The presence of GB affects water structure. The $O_w-O_w$ RDFs in water and water−GB mixtures (Figure 4B) show their first peak at 0.28 nm for hydrogen-bonded first neighbors and their second peak at 0.45 nm corresponding to the tetrahedrally located second neighbors. Similar observations have been made by Wei et al.[82] in their work on osmolytes. The presence of GB enhances the height of first peak and increases the depth of the first minimum, suggesting enhancement of water structure by GB. The location of peaks and heights in the RDF of water match with the earlier reported values.[46] Addition of GB in water has an effect similar to that of addition of urea in the case of methane molecules. This synergistic effect of GB can be further explained by analyzing hydrogen bond properties in the water−GB mixture. The addition of GB reduces the average number of hydrogen bonds per water molecule (Table 9) as the number density of water decreases considerably but increases the lifetimes of hydrogen bonds (Table S5, Supporting Information). Similar observations have been reported earlier for aqueous solution of osmolytes, where enhancements in the lifetimes of hydrogen bonds have been found.[40,82,92]

**4.3. Water−Urea.** The presence of urea in water enhances the hydrophobic association of methane. This is supported by other simulation results as well.[24,52−54,57] The appearance of a contact minimum at 0.39 nm with an increase in depth suggests the enhancement of methane clustering/association. The PMF curve (blue curve in Figure 2) also shows the existence of solvent-separated minimum at 0.72 nm corresponding to hydrophobic solvation of methane molecules. The two states are separated by an energy barrier of 1.2 kJ $mol^{-1}$ (Figure 2). The decrease in the value of the equilibrium constant for methane molecules in aqueous urea is consistent with this observation. The enhanced clustering of methane by urea is supported by the equilibrium constant for methane molecules in aqueous urea (Table 3). When methane molecules approach the contact minimum from transition state, the values of $\Delta H$ become more positive and values of $-T\Delta S$ become more negative because there is a removal of larger number of water molecules from the coordination shell of methane. The $T\Delta S$ term is the largest for water urea mixture in the CM region.

The clustering of solute molecules due to hydrophobic association reduces contact between solutes and solvent. This helps in maintaining uniform distribution of urea in water.[52−54] Besides, hydrophobic solvation requires the creation of a cavity. The work that needs to be done for cavity creation in urea is larger than that in water (Table 4). The presence of solute clusters in neat water suggests that urea does not necessarily initiate methane clustering but enhances it when added to water.

The creation of suitable sized cavities to hold solutes requires flexibility in a solvent, which depends on the solvent−solvent interaction. This molecular scale flexibility is a major contributor in cavity creation and hence the hydrophobic solvation. According to van der Vegt et al.,[53] it may also determine the magnitude and sign of the solute−solvent entropy change when a solute is transferred from one solvent to another.

In the aqueous urea mixture, the association of methane, i.e., "salting out" is driven by entropy and disfavored by enthalpy.

We observe that in aqueous urea mixture (Figure 4C), methane−methane interaction is stronger than methane−water and methane−urea interactions, which leads to enhanced



DOI: 10.1021/acs.jpcb.5b00556
J. Phys. Chem. B XXXX, XXX, XXX−XXX

clustering/association. RDF curves also show preferential solvation of methane by water. The excess coordination numbers (ECNs) of water and urea molecules around methane in aqueous urea support these observations (Figure S6, Supporting Information). van Gunsteren and co-workers[54] have reported similar observations in their work. A possible mechanism for this behavior is that methane molecules are being pushed away from urea into water, thereby increasing the local concentration of methane in water, leading to likely enhanced clustering. This is due to preferential solvation of methane by water over urea. The values of running coordination numbers calculated in the first coordination shell of methane in aqueous urea mixture support this. At room temperature, the solvation free energy of methane is 9.7 kJ $mol^{-1}$ in water−urea, which shows that methane is less soluble in urea than in water. In the presence of urea, hydrophobic association of methane is enhanced, which is also supported by solvation free energy data (Table 4). The preferential binding constant ($\nu$ in favor of urea) for methane in water−urea is −1.19. This too suggests preferential solvation by water. Analysis of RDF of $O_w$−$O_w$ and lifetimes of hydrogen bonds shows that addition of urea enhances local structure of water and hydrogen bond lifetimes. The number of hydrogen bonds per water molecule decreases from 3.75 in water to 2.96 in water−urea. The considerable decrease in the number density of water in the mixture is responsible for this decrease.

**4.4. Water−Urea−GB.** Urea is a denaturing osmolyte whereas GB is protecting in nature. In aqueous urea, a "salting-in" effect for larger hydrocarbons is favored by the van der Waal's interaction energy. However, in the case of methane, addition of urea causes a "salting-out" effect.[24,52−54]

As suggested by van Gunsteren and co-workers,[54] this is perhaps due to the fact that the solute molecules are being pushed away from urea into water, thereby increasing the local concentration of methane in water. This leads to enhancement of clustering. The work involved in the cavity creation in urea is larger than that in water (solvation free energy data given in Table 4). Analysis of RDFs of $O_w$−$O_w$ shows that addition of urea enhances the first peak (Figure 5). Addition of GB also strengthens the structure of water as described earlier. This leads to salting out of methane. The value the of equilibrium constant obtained supports this observation.

In the mixture of water−urea−GB, the contact minimum is stabilized by entropy and favored by enthalpy because, when methane molecules approach the contact minimum, there is removal of water, urea, and GB molecules from the coordination shells of methane. When the CM is approached from the transition state, the entropy contribution monotonically decreases, whereas the enthalpy contribution initially increases and finally reaches a local minimum at the CM. These features are similar to those for water and water−GB mixtures. The solvent-separated minimum is also strongly stabilized by entropy and favored by enthalpy.

The number of hydrogen bonds per water molecule decreases on the addition of GB to aqueous urea containing methane molecules as the number density of water decreases significantly. From the analysis of RCNs, KBIs, and ECNs, we note that methane prefers water over GB and urea in an aqueous urea−GB mixture. Therefore, both urea and GB are excluded from the methane surface, which suggests that both urea and GB tend to salt out methane. This is one of the major findings of the paper. The solubility of methane is least in the mixture, which is reflected by the solvation free energies of methane given in Table 4. The enhancement of water structure in this mixture is also supported by very low values of the diffusion constants.

## 5. CONCLUSIONS

Hydrophobic association and solvation of methane molecules in aqueous solutions of urea and GB have been studied using MD simulations. We have calculated the potentials of mean force between methane molecules in water, aqueous GB, aqueous urea, and aqueous urea−GB mixtures. The PMFs obtained distinctly show enhancement of methane association on the addition of these osmolytes. These observations are well supported by calculation of equilibrium constants. Association of methane is dominated by entropy and solvation of methane is favored by enthalpy in all the mixtures. In the water−urea−GB mixture, hydrophobic association and solvation are both stabilized by entropy. The calculated solvation free energies of methane in these mixtures show that methane is less soluble in the mixtures of urea and GB than in water. The solubility is the least in the water−urea−GB mixture.

Analysis of RDFs suggests that addition of both the osmolytes enhances local water structure. The values of diffusion constants obtained for water support the strong association of water with urea and GB. Besides RDFs, we have also calculated RCNs and ECNs of solvent and cosolvent around methane molecules to understand preferential solvation of methane. Such studies provide an insight into "salting in" and "salting out" of solute molecules. We find that both urea and GB are preferentially excluded from the methane surface in the mixtures of osmolytes because of the strong association between water−GB and water−urea. Therefore, methane is preferentially solvated by water molecules in the mixtures of osmolytes. The favorable exclusions of both urea and GB from the methane surface suggest that both urea and GB increase the association of methane molecules, i.e., salting-out of methane. It is interesting that the osmolytes in our studies, namely, urea and GB, belong to different classes that show opposite effects on association and solvation of larger molecules. It would be desirable to study larger alkanes and biological entities such as proteins in aqueous mixtures containing different combinations of osmolytes. Studies of such systems will assist in understanding the mechanism of important physical processes of solubility and the role of osmolytes in stabilizing and denaturing proteins.

## ■ ASSOCIATED CONTENT

### Supporting Information

Lists of partial charges on the glycine−betaine molecule, positions and free energies of contact minima, transition state, and solvent-separated minima, running coordination numbers of water molecules in the first coordination shell of urea and GB, preferential binding constants ($\nu$) of methane with methyl sites of GB in the $II_{w\text{-}GB}$ mixture, and lifetimes of hydrogen bonds of water molecule in the bulk in $I_w$, $II_{w\text{-}GB}$, $III_{w\text{-}ua}$, and $IV_{w\text{-}ua\text{-}GB}$. Figures showing potential man force of methane molecules in $I_w$, $II_{w\text{-}GB}$, $III_{w\text{-}ua}$, and $IV_{w\text{-}ua\text{-}GB}$, radial distribution functions of methane with each site of glycine−betaine in the water−GB mixture and with each site of urea in the water−urea mixture, radial distribution functions between GB and water, excess coordination numbers of water, urea, and GB molecules around methane, and hydrogen bond time correlation functions in water, water−GB, water−urea, and water−urea−GB solutions. The Supporting Information is available free of



DOI: 10.1021/acs.jpcb.5b00556
J. Phys. Chem. B XXXX, XXX, XXX−XXX

charge on the ACS Publications website at DOI: 10.1021/acs.jpcb.5b00556.

## AUTHOR INFORMATION


### Corresponding Author

*B. L. Tembe. Phone No.: +91-22-2576-4199. Fax No.: +91-22-2576-7152. E-mail: bltembe@chem.iitb.ac.in.


### Notes

The authors declare no competing financial interest.

## ACKNOWLEDGMENTS

We express our gratitude to IIT Bombay for providing us with the High Performance Computing Facility and the Department of Chemistry, IIT Bombay, for providing research facilities. M.K.D. thanks UGC, Government of India, for a Senior Research Fellowship. A.A.S. thanks UGC for providing support in pursuing research. We thank Timir Hajari for fruitful discussions.

## REFERENCES


(1) Kauzmann, W. Some Factors in the Interpretation of Protein Denaturation. *Adv. Protein Chem.* **1959**, *14*, 1−63.

(2) Dill, K. A. Dominant Forces in Protein Folding. *Biochemistry* **1990**, *29*, 7133−7155.

(3) Tanford, C. *The Hydrophobic Effect: Formation of Micelles and Biological Membranes*; John Wiley: New York, 1973.

(4) Chandler, D. Interfaces and the Driving Force of Hydrophobic Assembly. *Nature* **2005**, *437*, 640−647.

(5) Choudhury, N.; Pettitt, B. M. The Dewetting Transition and the Hydrophobic Effect. *J. Am. Chem. Soc.* **2007**, *129*, 4847−4852.

(6) Tanford, C. How Protein Chemists Learned About the Hydrophbic Factors. *Protein Sci.* **1997**, *6*, 1358−1366.

(7) Caballero-Herrera, A.; Nordstrand, K.; Berndt, K. D.; Nilsson, L. Effect of Urea on Peptide Conformation in Water: Molecular Dynamics and Exprimental Characterization. *Biophys. J.* **2005**, *89*, 842−857.

(8) Timasheff, S. N. The Control of Protein Stability and Association by Weak Interactions with Water: How Do Solvents Affect These Processes. *Annu. Rev. Biophys. Biomol. Struct.* **1993**, *22*, 67−97.

(9) Bolen, D. W.; Rose, G. D. Structure and Energetics of the Hydrogen-Bonded Backbone in Protein Folding. *Annu. Rev. Biochem.* **2008**, *77*, 339−362.

(10) Stewart, J. A.; Ouellet, L. A. Stopped-Flow Mixing Device for the Spectrophotometric Study of Rapid Reactions. *Can. J. Chem.* **1959**, *37*, 744−750.

(11) Brown, A. D.; Simpson, J. R. Water Relations of Sugar-Tolerant Yeasts: The Role of Intracellular Polyols. *J. Gen. Microbiol.* **1972**, *72*, 589−591.

(12) Bennion, B. J.; Daggett, V. The Molecular Basis for the Chemical Denaturation of Proteins by Urea. *Proc. Natl. Acad. Sci. U. S. A.* **2003**, *100*, 5142−5147.

(13) Idrissi, A.; Cinar, E.; Longelin, S.; Damay, P. The Effect of Temperature on Urea-Urea Interactions in Water: a Molecular Dynamics Simulation. *J. Mol. Liq.* **2004**, *110*, 201−208.

(14) Watlaufer, D. B.; Malik, S. K.; Stoller, L.; Coffin, R. L. Nonpolar Group Participation in the Denaturation of Proteins by Urea and Guanidinium Salts. Model Compound Studies. *J. Am. Chem. Soc.* **1964**, *86*, 508−514.

(15) Frank, H. S.; Franks, F. Structural Approach to the Solvent Power of Water for Hydrocarbons; Urea as a Structure Breaker. *J. Chem. Phys.* **1968**, *48*, 4746−4757.

(16) Finer, E. G.; Franks, F.; Tait, M. J. Nuclear Magnetic Resonance Studies of Aqueous Urea Solutions. *J. Am. Chem. Soc.* **1972**, *94*, 4424−4429.

(17) Vanzi, F.; Madan, B.; Sharp, K. Effect of the Protein Denaturant Urea and Guanidinium on Water Structure: A Structural and Thermodynamic Study. *J. Am. Chem. Soc.* **1998**, *120*, 10748−10753.

(18) Das, A.; Mukhopadhyay, C. Urea-Mediated Protein Denaturation: A Consensus View. *J. Phys. Chem. B* **2009**, *113*, 12816−12824.

(19) Nozaki, Y.; Tanford, C. The Solubility of Amino Acids and Related Compounds in Aqueous Urea Solutions. *J. Biol. Chem.* **1963**, *238*, 4074−4081.

(20) Robinson, D. R.; Jencks, W. P. The Effect of Compounds of the Urea-Guanidinium Class on the Activity Coefficient of Acetyltetraglycine Ethyl Ester and Related Compounds. *J. Am. Chem. Soc.* **1965**, *87*, 2462−2470.

(21) Alonso, D. O. V.; Dill, K. A. Solvent Denaturation and Stabilization of Globular Proteins. *Biochemistry* **1991**, *30*, 5974−5985.

(22) Makhatadze, G. I.; Privalov, P. L. Protein Interactions with Urea and Guanidinium Chloride: A Calorimetric Study. *J. Mol. Biol.* **1992**, *226*, 91−505.

(23) Mountain, R. D.; Thirumalai, D. Molecular Dynamics Simulations of End-to-End Contact Formation in Hydrocarbon Chains in Water and Aqueous Urea Solution D. *J. Am. Chem. Soc.* **2003**, *125*, 1950−1957.

(24) Wallqvist, A.; Covell, D. G.; Thirumalai, D. Hydrophobic Interactions in Aqueous Urea Solutions with Implications for the Mechnism of Protein Denaturation. *J. Am. Chem. Soc.* **1998**, *120*, 427−428.

(25) O'Brein, E. P.; Dima, R. I.; Brooks, B.; Thirumalai, D. Interactions Between Hydrophobic and Ionic Solutes in Aqueous Guanidinium Chloride and Urea Solutions: Lessons for Protein Denaturation Mechanism. *J. Am. Chem. Soc.* **2007**, *129*, 7346−7353.

(26) Lee, M. E.; van der Vegt, N. F. A. Does Urea Denature Hydrophobic Interactions? *J. Am. Chem. Soc.* **2006**, *128*, 4948−4949.

(27) Hua, L.; Zhou, R.; Thirumalai, D.; Berne, B. J. Urea Denaturation by Stronger Dispersion Interactions with Proteins than Water Implies a 2-Stage Unfolding. *Proc. Natl. Acad. Sci. U. S. A.* **2008**, *105*, 16928−16933.

(28) Zangi, R.; Zhou, R.; Berne, B. J. Urea's Action on Hydrophobic Interactions. *J. Am. Chem. Soc.* **2009**, *131*, 1535−1541.

(29) Stumpe, M. C.; Grubmller, H. Urea Impedes the Hydrophobic Collapse of Partially Unfolded Proteins. *Biophys. J.* **2009**, *96*, 3744−3752.

(30) Lim, W. K.; Rösgen, J.; Englander, S. W. Urea, but not Guanidinium, Destabilizes Proteins by Forming Hydrogen Bonds to the Peptide Group. *Proc. Natl. Acad. Sci. U. S. A.* **2009**, *106*, 2595−2600.

(31) Wang, A.; Bolen, D. W. A Naturally Occurring Protective System in Urea-Rich Cells: Mechanism of Osmolyte Protection of Proteins against Urea Denaturation. *Biochemistry* **1997**, *36*, 9101−9108.

(32) Liu, Y.; Bolen, D. W. The Peptide Backbone Plays a Dominat Role in Protein Stabilization by Naturally Occurring Osmolytes. *Biochemistry* **1995**, *34*, 12884−12891.

(33) Baskakov, I.; Bolen, D. W. Forcing Thermodynamics Unfold Protein to Fold. *J. Biol. Chem.* **1998**, *273*, 4831−4834.

(34) Bolen, D. W.; Baskakov, I. V. The Osmophobic Effect: Natural Selection of a Thermodynamic Force in Protein Folding. *J. Mol. Biol.* **2001**, *310*, 955−963.

(35) Zou, Q.; Bennion, B. J.; Daggett, V.; Murphy, K. P. The Molecular Mechanism of Stabilization of Proteins by TMAO and Its Ability to Counteract the Effects of Urea. *J. Am. Chem. Soc.* **2002**, *124*, 1192−1202.

(36) Aburi, M.; Smith, P. E. A Combined Simulation and Kirkwood-Buff Approach to Quantify Cosolvent Effects on the Conformational references of Peptides in Solution. *J. Phys. Chem. B* **2004**, *108*, 7382−7388.

(37) Shimizu, S. Estimating Hydration Changes upon Biomolecular Reactions from Osmotic Stress, High Pressure, and Preferential Hydration Experiments. *Proc. Natl. Acad. Sci. U. S. A.* **2004**, *101*, 1195−1199.

(38) Paul, S.; Patey, G. N. Structure and Interaction in Aqueous Urea Trimethylamine-N-oxide Solutions. *J. Am. Chem. Soc.* **2007**, *129*, 4476−4482.




DOI: 10.1021/acs.jpcb.5b00556
J. Phys. Chem. B XXXX, XXX, XXX−XXX

(39) Jiao, Y.; Smith, P. E. Fluctuation Theory of Molecular Association and Conformational Equilibria. *J. Chem. Phys.* **2011**, *135*, 014502−014512.
(40) Bennion, B. J.; Daggett, V. Counteraction of Urea-Induced Protein Denaturation by Trimethylamine N-Oxide: A Chemical Chaperone at Atomic Resolution. *Proc. Natl. Acad. Sci. U. S. A.* **2004**, *101*, 6433−6438.
(41) Rose, G.; Fleming, P.; Banavar, J.; Maritan, A. A Backbone-Based theory of Protein Folding. *Proc. Natl. Acad. Sci. U. S. A.* **2006**, *103*, 16623−16633.
(42) Canchi, D. R.; Jayasimha, P.; Rau, D. C.; Makhatadze, G. I.; García, A. E. Molecular Mechanism for the Preferential Exclusion of TMAO from Protein Surfaces. *J. Phys. Chem. B* **2012**, *116*, 12095−12104.
(43) Canchi, D. R.; García, A. E. Cosolvent Effects on Protein Stability. *Annu. Rev. Phys. Chem.* **2013**, *64*, 273−293.
(44) Ganguly, P.; Hajari, T.; Shea, J. E.; van der Vegt, N. F. A. Mutual Exclusion of Urea and Trimethylamine N-Oxide from Amino Acids in Mixed Solvent Environment. *J. . Phys. Chem. Lett.* **2015**, *6*, 581−585.
(45) Moeser, B.; Horinek, D. The Role of the Concentration Scale in the Definition of Transfer Free Energies. *Biophysical Chem.* **2015**, *196*, 68−76.
(46) Venkatesu, P.; Lee, M. J.; Lin, H. Osmolytes Counteracts Urea-Induced Denaturation of $\alpha$-Chymotrypsin. *J. Phys. Chem. B* **2009**, *113*, 5327−5338.
(47) Kumar, N.; Kishore, N. Synergistic Behavior of Glycine Betaine-Urea Mixture: A Molecular Dynamics Study. *J. Chem. Phys.* **2013**, *139*, 115104−115109.
(48) Kumar, N.; Kishore, N. Protein Stabilization and Counteraction of Denaturing Effect of Urea by Glycine Betaine. *Biophysical Chem.* **2014**, *189*, 16−24.
(49) Shimizu, S.; Chan, H. S. Configuration-Dependent Heat Capacity of Pairwise Hydrophobic Interactions. *J. Am. Chem. Soc.* **2001**, *123*, 2083−2084.
(50) Shimizu, S.; Chan, H. S. Anti-Cooperativity and Cooperativity in Hydrophobic Interactions: Three-Body Free Energy Landscapes and Comparison with Implicit-Solvent Potential Functions for Proteins. *Proteins* **2002**, *48*, 15−30.
(51) Shimizu, S.; Chan, H. S. Origin of Protein Denatured State Compactness and Hydropphobic Clustering in Aqueous Urea: Inferences from Nonpolar Potentials of Mean Force. *Proteins* **2002**, *49*, 560−566.
(52) Ikeguchi, M.; Nakamura, S.; Shimizu, K. Molecular Dynamics Study on Hydrophobic Effects in Aqueous Urea Solutions. *J. Am. Chem. Soc.* **2001**, *123*, 677−682.
(53) Trzesniak, D.; van der Vegt, N. F. A.; van Gunsteren, W. F. Computer Simulation Studies on the Solvation of Aliphatic Hydrocarbons in 6.9M Aqueous Urea Solution. *Phys. Chem. Chem. Phys.* **2004**, *6*, 697−702.
(54) Oostenbrink, C.; van Gunsteren, W. F. Methane Clustering in Explicit Water: Effect of Urea on Hydrophobic Interactions. *Phys. Chem. Chem. Phys.* **2005**, *7*, 53−58.
(55) Athawale, M. V.; Sarupria, S.; Garde, S. Ehthalpy-Entropy Contributions to Salts and Osmolytes Effects on Molecular-Scale Hydrophobic Hydration and Interactions. *J. Phys. Chem. B* **2008**, *112*, 5661−5670.
(56) Ghosh, T.; Garcia, A. E.; Garde, S. Enthalpy and Entropy Contributions to the Pressure Dependence of Hydrophobic Interactions. *J. Chem. Phys.* **2002**, *116*, 2480−2486.
(57) Sarma, R.; Paul, S. Association of Small Hydrophobic Solute in Presence of the Osmolytes Urea and Trimethylamine-N-oxide. *J. Phys. Chem. B* **2012**, *116*, 2831−2841.
(58) Hess, B.; Kutzner, C.; van der Spoel, D.; Lindahl, E. GROMACS 4: Algorithms for Highly Efficient, Load-Balanced, and Scalable Molecular Simulation. *J. Chem. Theory Comput.* **2008**, *4*, 435−447.
(59) Essmann, U.; Perera, L.; Berkowitz, M. L.; Darden, T.; Lee, H.; Pedersen, L. G. A. Smooth Particle Mesh Ewald Method. *J. Chem. Phys.* **1995**, *103*, 8577−8593.
(60) Berendsen, H. J. C.; Postma, J. P. M.; van Gunsteren, W. F.; DiNola, A.; Haak, J. R. Molecular Dynamics with Coupling to an External Bath. *J. Chem. Phys.* **1984**, *81*, 3684−3690.
(61) Hess, B.; Bekker, H.; Berendsen, H. J. C.; Fraaije1, J. G. E. M. LINCS: A Linear Constraint Solver for Molecular Simulations. *J. Comput. Chem.* **1997**, *18*, 1463−1472.
(62) Bussi, G.; Donadio, D.; Parrinello, M. Canonical Sampling through Velocity Rescaling. *J. Chem. Phys.* **2007**, *126*, 014101−014107.
(63) Berendsen, H. J. C.; Grigera, J. R.; Straatsma, T. P. J. The Missing Term in Effective Pair Potentials. *J. Phys. Chem.* **1987**, *91*, 6269−6271.
(64) Jorgensen, W. L.; Maxwell, D. S.; Tirado-Rives, J. Development and Testing of the OPLS All-Atom Force Field on Conformational Energetics and Properties of Organic Liquids. *J. Am. Chem. Soc.* **1996**, *118*, 11225−11236.
(65) Jorgensen, W. L.; McDonald, N. A. Development of An All-Atom Force Field for Heterocycles. Properties of Liquid Pyridine and Diazenes. *THEOCHEM* **1998**, *424*, 145−155.
(66) Jorgensen, W. L.; McDonald, N. A. Development of an All-Atom Force Field for Heterocycles. Properties of Liquid Pyrrole, Furan, Diazoles, and Oxazoles. *J. Phys. Chem. B* **1998**, *102*, 8049−8059.
(67) Rizzo, R. C.; Jorgensen, W. L. OPLS All-Atom Model for Amines: Resolution of the Amine Hydration Problem. *J. Am. Chem. Soc.* **1999**, *121*, 4827−4836.
(68) Price, M. L.; Ostrovsky, D.; Jorgensen, W. L. Gas-Phase and Liquid-State Properties of Esters, Nitriles, and Nitro Compounds with the OPLS-AA Force Field. *J. Comput. Chem.* **2001**, *22*, 1340−1352.
(69) Watkins, E. K.; Jorgensen, W. L. Perfluoroalkanes: Conformational Analysis and Liquid-State Properties from AB Initio and Monte Carlo Calculations. *J. Phys. Chem. A* **2001**, *105*, 4118−4125.
(70) Kaminski, G. A.; Friesner, R. A.; Tirado-Rives, J.; Jorgensen, W. L. Evaluation and Reparametrization of the OPLS-AA Force Field for Proteins via Comparison with Accurate Quantum Chemical Calculations on Peptides. *J. Phys. Chem. B* **2001**, *105*, 6474−6487.
(71) Frisch, M. J.; Trucks, G. W.; Schlegel, H. B.; et al. *Gaussian 09*, Revision A.02; Gaussian, Inc.: Wallingford, CT, 2009.
(72) Kahn, K.; Bruice, T. C. Parameterization of OPLS−AA Force Field for the Conformational Analysis of Macrocyclic Polyketides. *J. Comput. Chem.* **2002**, *23*, 977−996.
(73) Jorgensen, W. L.; Gao, J. J. Monte Carlo Simulations of the Hydration of Ammonium and Carboxylate Ions. *J. Phys. Chem.* **1986**, *90*, 2174−2182.
(74) Singh, U. C.; Kollman, P. A. An Approach to Computing Electrostatic Charges for Molecules. *J. Comput. Chem.* **1984**, *5*, 129−145.
(75) Shek, Y. L.; Chalikian, T. V. Volumetric Charactrization of Interaction of Glycine Betaine with Protein Groups. *J. Phys. Chem. B* **2011**, *115*, 11481−11489.
(76) Martinez, L.; Andrade, R.; Birgin, E. G.; Martinez, J. M. Packmole: A Package for Building Initial Configurations for Molecular Dynamics Simulations. *J. Comput. Chem.* **2009**, *30*, 2157−2164.
(77) Parrinello, M.; Rahman, A. Polymorphic Transitions in Single Crystals: A New Molecular Dynamics Method. *J. Appl. Phys.* **1981**, *52*, 7182−7190.
(78) Nose, S.; Klein, M. L. Constant Pressure Molecular Dynamics for Molecular Systems. *Mol. Phys.* **1983**, *50*, 1055−1076.
(79) Peter, C.; Oostenbrink, C.; van dorp, A.; van Gunsteren, W. F. Estimating Entropies from Molecular Dynamics Simulations. *J. Chem. Phys.* **2004**, *120*, 2652−2661.
(80) Ben-Naim, A. *Solvation Thermodynamics*; Plenum Press: New York, 1987.
(81) Widom, B. Some Topics in the Theory of Fluids. *J. Chem. Phys.* **1963**, *39*, 2808−2812.
(82) Wei, H.; Fan, Y.; Gao, Y. Q. Effects of Urea, Tetramethyl Urea and Trimethylamine N-Oxide on Aqueous Solution Structure and Solvation of Protein Backbones: A molecular Dynamics Simulation Study. *J. Phys. Chem. B* **2010**, *114*, 557−568.


DOI: 10.1021/acs.jpcb.5b00556
*J. Phys. Chem. B* XXXX, XXX, XXX−XXX

(83) Kirkwood, J. G.; Buff, F. P. The Statistical Mechanical Theory of Solutions. 1. *J. Chem. Phys.* **1951**, *19*, 774−777.
(84) Schurr, J. M.; Rangel, D. P.; Aragon, S. R. A Contribution to the Theory of Preferential Interaction Coefficients. *Biophys. J.* **2005**, *89*, 2258−2276.
(85) Ganguly, P.; van der Vegt, N. F. A. Convergence of Sampling Kirkwood−Buff Integrals of Aqueous Solutions with Molecular Dynamics Simulations. *J. . Chem. Theory. Chomput.* **2013**, *9*, 1347−1355.
(86) Ganguly, P.; Hajari, T.; van der Vegt, N. F. A. Molecular Simulation Study on Hofmeister Cations and the Aqueous Solubility of Benzene. *J. . Phys. Chem. B* **2014**, *118*, 5331−5339.
(87) Schnell, S. K.; Liu, X.; Simon, J.-M.; Bardow, A.; Bedeaux, D.; Vlugt, T. J. H.; Kjelstrup, S. Calculating Thermodynamic Properties from Fluctuations at Small Scales. *J. Phys. Chem. B* **2011**, *115*, 10911−109918.
(88) Eastea, A. J. Tracer Diffusion in Aqueous Sucrose and Urea Solutions. *Can. J. Chem.* **1990**, *68*, 1611−1615.
(89) Luzar, A.; Chandler, D. Hydrogen-Bond Kinetics in Liquid Water. *Nature* **1996**, *379*, 55−57.
(90) Southall, N. T.; Dill, K. A. Potential of Mean Force between Two Hydrophobic Solutes in Water. *Biophys. Chem.* **2002**, *101*, 295−307.
(91) Stillinger, F. H. Structure in Aqueous Solutions of Nonpolar Solutes from the Standpoint of Scaled-Particle Theory. *J. Solution Chem.* **1973**, *2*, 141−158.
(92) Athawale, M. V.; Dordick, J. S.; Garde, S. Osmolyte Trimethylamine-N-Oxide Does Not Affect the Strength of Hydrophobic Interactions: Origin of Osmolyte Compatibility. *Biophys. J.* **2005**, *89*, 858−866.


DOI: 10.1021/acs.jpcb.5b00556
*J. Phys. Chem. B* XXXX, XXX, XXX−XXX